DOI: 10.13009/EUCASS2023-861
Aerospace Europe Conference 2023 – 10TH EUCASS – 9TH CEAS

Particle-based modeling of the unsteady flow in a high-test peroxide catalytic chamber

Nora M. Bierwagen[1], Stefan May[1], Thino Eggers[2], Andreas Ohndorf [1] and Christian Mundt[3]*
[1] Responsive Space Cluster Competence Center, German Aerospace Center (DLR)
Fassberg, Germany
[2] Institute of Aerodynamics and Flow Technology, German Aerospace Center (DLR)
Braunschweig, Germany
[3] Faculty of Aerospace Technology, Institute for Thermodynamics, Universität der Bundeswehr München
Neubiberg, Germany
nora.bierwagen@dlr.de – stefan.may@dlr.de – thino.eggers@dlr.de – andreas.ohndorf@dlr.de – christian.mundt@unibw.de
[*] Corresponding Author

Abstract
A particle-based mathematical model is proposed. It contains a one-dimensional approximation of the flow with heat transfer in the chamber wall and the catalytic material. It is designed for packed bed reactors with spherical granulated catalytic materials and is customized for high-test peroxide as fluid. The unsteady flow in the cold start phase can be analyzed. The temperature values increase over the time and the mass fraction of the chemical components are useable for a better understanding of the process inside and a precise design of new catalytic chambers with an improved functionality.

1. Introduction

In the last years hydrogen peroxide (H_2O_2) gains in importance as a “green” rocket propellant, because of its nontoxic properties and the decomposition to pollution-free components. Hence, for monopropellant engines it is an environmentally friendly alternative propellant. The storage suitability over a long time and the safety in the direct handling (nontoxic, noncarcinogen) are further advantages [1, 2]. For hybrid rocket engines it has in combination with hydroxyl-terminated polybutadiene (HTPB) the benefit that the specific impulse over the oxidiser-fuel ratio gives a flat curve. Out of it the active regulation of the thrust is possible in an attractive range. Because hydrogen peroxide is not cryogenic, it is an appropriate alternative to liquid oxygen. The main advantage of hydrogen peroxide is the possibility to waive on additional ignition systems which makes the ignition process reliable. In contact with some materials, for example Platin, it decomposes exothermically to oxygen (O_2) and water vapour (H_2O) [2]. This steam heats up the HTPB and start the combustion process without additional ignition systems. In addition, the catalytic chamber assures a homogenous combustion process within the combustion chamber. The chemical decomposition process takes place in catalytic chambers.
The department Spacecraft of the DLR Institute of Aerodynamics and Flow Technology developed the software tool AHRES (Advanced Hybrid Rocket Engine Simulation) [3, 4]. It is a pre-design software for complete hybrid rocket engines. The calculations of the software are validated with experimental data from ground tests at the DLR site Trauen (Germany) and numerical simulations of the inner flow and combustion with the DLR TAU-Code. The submodule SHAKIRA (Simulation of High-test peroxide Advanced C(K)atalytic Ignition system for Rocket Applications) calculates the decomposition process inside the catalytic chamber of a hybrid rocket engine [5]. For the validation experimental data from different catalytic chambers are available [6]. To date a mass flow of 4.5 kg/s in the catalytic chamber is the maximum which was tested at the testbench with a cold start procedure.
In literature several decomposition models of catalytic chambers with hydrogen peroxide exist. In the following some important models will be presented. Pasini et al. [7] introduce a steady state, one-dimensional homogenous flow model with a decomposition model which respects the adsorption and desorption processes. They investigate the general behaviour by the variation of basic parameters. Later the model of Pasini et al. was used by other research groups and modified in some ways. Jung et al. [8] alter the model to consider the particle size. Therefore, an equation which connects the particle size to the porosity is added. Then the results are compared to experimental data. They found

DOI: 10.13009/EUCASS2023-861

deviations in the pressure description [8]. Kerr et al. [9] make an uncertainty analysis of the parameter in the model. For every input parameter a Gaussian distribution is allocated. The sensitivity analysis shows that the propellant mass fraction is the most sensitive parameter [9]. Another model is presented by Koopmanns et al. [10]. It is a one-dimensional heterogenous model which considers the liquid and gas phase separately, but it has a deficit in the treatment from the heat transfer between the particle and the fluid. The decomposition model respects the adsorption and desorption processes too. Reid et al. [11] shows a steady state, one-dimensional heterogenous model which separate the particle and the mixture fluid flow. For the decomposition process the diffusional limitations are considered. The model of Reid et al. is not yet been validated with experimental data.
All presented models in the literature have a main similarity: the spatial treatment. The models above divide the space in equal discrete volumes. The idea of SHAKIRA is to model the space with a particle-based approach. Thereby, the unsteady flow in the cold start phase of the catalytic chamber can be modelled. This is a very important transient behaviour of a catalytic chamber. Its understanding is essential for the optimal design of the catalytic chamber to achieve the best performance. Furthermore, the model considers the heat exchange between the solid catalytic particles and the fluid. Also, a two-dimensional heat equation in the catalytic chamber wall is solved for the heat transfer between the wall and the fluid.

2. Flow Model

2.1 General Features

In the catalytic chamber the hydrogen peroxide is upstream in liquid state, then it is partially liquid and partially gaseous and downstream it is fully gaseous. Therefore, the flow cannot be treated as a single-phase flow. It is a multiphase flow, which consists simultaneous of several phases and molecules [12]. In the special case of two different phases, such flows can be designated as two-phase flow. The simplest method to model such flows is the homogenous flow theory [12]. It treats the fluid as pseudo fluid with averaged properties. This approach is used in this paper. Hence, the liquid and gaseous phase of high-test peroxide are modelled as mixed fluid. The solid catalytic particles are simulated as spatially fixed.
For a better simulation of the cold start phase of the catalytic chamber, the one-dimensional particle-based approach is used. Therefore, the radial extension of the slices in the catalytic chamber is reduced to one particle. Each particle has averaged properties for the space which it represents. The space of each particle depends on the own velocity. An example particle formation can be seen in figure 1.

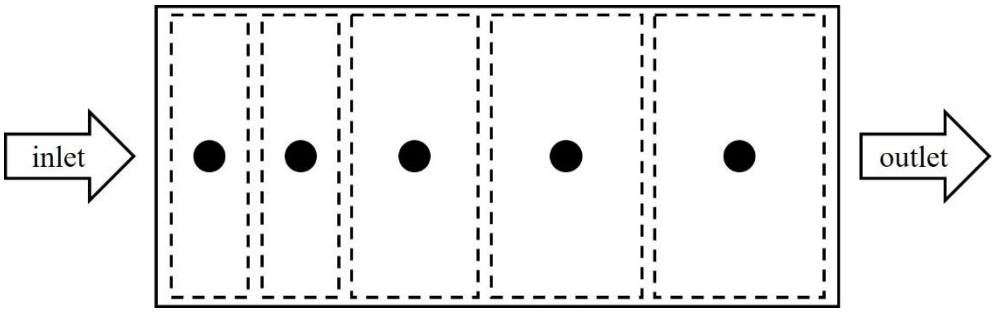

Figure 1: Schematically drawing of the flow model

SHAKIRA is a submodule coded in the language python. It has one loop for the time progress and a sequence of calculations for each time step. A flow chart of this sequence is shown in figure 2. First, each time step starts with the calculation of the new mass fractions as result of the chemical decomposition. Then, the new fluid temperature of each particle is computed. Following the pressure drop can be calculated. Moreover, the flow parameter like density, heat capacity and thermal conductivity are worked out. Finally, the heat conduction in the wall and the resulting heat flux are calculated. In the following the detailed mathematical modelling of the different parts of the sequence are explained.

DOI: 10.13009/EUCASS2023-861

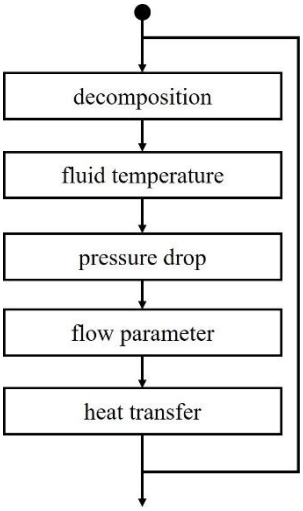

Figure 2: Sequence of the calculations for each time step

2.2 Detailed Mathematical Modelling

For the one-dimensional mixture model the equations for mass, momentum and energy conservation are the same as for a single-phase flow just mixture properties have to be used. The differential form of the conservation equations is the following [13]:

$$\frac{\partial \rho_m}{\partial t} + \frac{\partial \rho_m v_m}{\partial x} = 0 \tag{1}$$

$$\frac{\partial \rho_m v_m}{\partial t} + \frac{\partial \rho_m v_m^2}{\partial x} = -\frac{\partial p}{\partial x} + \frac{\partial \tau}{\partial x} \tag{2}$$

$$\frac{\partial \rho_m h_m}{\partial t} + \frac{\partial \rho_m h_m v_m}{\partial x} = -\frac{\partial q}{\partial x} \tag{3}$$

Here, ρ_m is the mixture density, v_m is the mixture velocity, t is the time, x is the space, p is the pressure, h_m is the mixture enthalpy and q is the heat flow. The shear stress τ is neglected. In the particle-based view the convective terms do not exist. Therefore, the equations simplify itself.

2.2.1 Decomposition

The catalytic decomposition of the liquid hydrogen peroxide to gaseous oxygen and water vapour follows the reaction equation [14]:

$$2H_2O_2 \rightarrow O_2 + 2H_2O + 196.14\ kJ/mol \tag{4}$$

It is an exothermic reaction which can be mathematically described with the Arrhenius equation [15]:

$$k = A\ exp\left(\frac{-E_a}{RT}\right) \tag{5}$$

DOI: 10.13009/EUCASS2023-861

Hereby, A is the pre-exponential factor, E_a is the activation energy which depends on the catalytic material, R the universal gas constant and T the temperature of the reactant. With the backward difference quotient, the change of mass fraction of hydrogen peroxide ΔH_2O_2 can be calculated from the differential equation [16]:

$$\boldsymbol{f(t, \{H_2O_2\}) = \frac{d\{H_2O_2\}}{dt}} \quad \textbf{(6)}$$

$$\boldsymbol{\Delta \{H_2O_2\} = \Delta t\, k_i\, [\{H_2O_2\}(t_{n-1})]^i \quad i \in (0, 1)} \quad \textbf{(7)}$$

Here, k is the velocity coefficient of the reaction, i is the reaction order and $\{\mathbf{H_2O_2}\}$ is the particle density of hydrogen peroxide. Pirault-Roy et al. [17] have shown that the reaction (1) with Platin catalyst is a first order reaction: $i = 1$.
It should be noted that the experimental determined velocity coefficient depends on the temperature, the catalytic material quantity and the catalytic material preparation. For the preparation the Brunauer-Emmett-Teller surface (BET) [18], is a common parameter. These three aspects got attention for the determining of the input values.
The micro kinetics mechanism of a heterogenous catalytic reaction like diffusion inside the porous particle and the adsorption and desorption mechanism [15] is not yet implemented in SHAKIRA. For further software versions it should be considered.

2.2.2 Fluid temperature

For the calculation of the fluid temperature the phase diagram is used. In figure 3, the phase diagram for a pressure of one bar is shown [19]. The pressure in catalytic chambers for rocket applications is usually higher than one bar. To overcome this shortcoming, the phase diagram has to be scaled with the pressure. The scaling factor is calculated with equation 8 [16]. The constants a, b and c (table 1) are computed with the findings of Coker [20].

$$\boldsymbol{s(p) = a\, p^b + c} \quad \textbf{(8)}$$

Table 1: Constants for the scaling factor in equation 8

	Value
a	0.3436
b	0.2102
c	0.6566

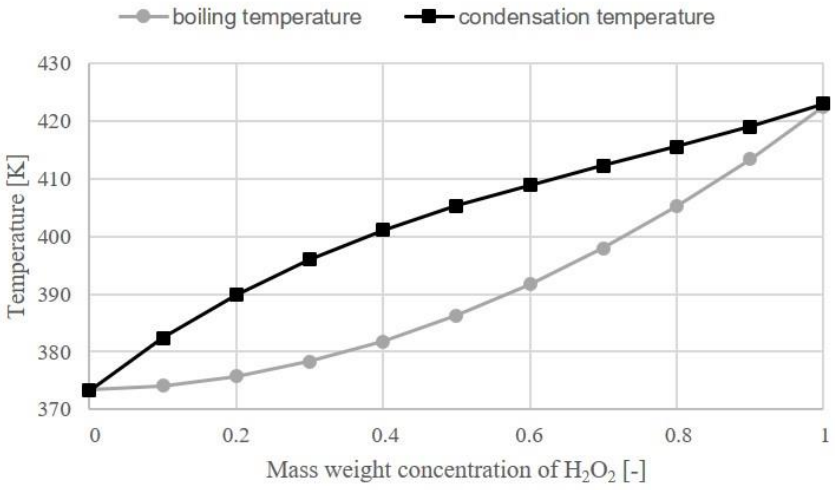

Figure 3: Phase diagram of hydrogen peroxide

DOI: 10.13009/EUCASS2023-861

With the knowledge of the enthalpy as well as the enthalpy of boiling and condensation for each particle, it can be ordered in the phase diagram. If the enthalpy is higher as the condensation enthalpy, the particle will be in the gaseous phase. If the enthalpy is lower as the boiling enthalpy, the particle will be in fluid phase. If the enthalpy is between the boiling and condensation enthalpy, the particle is in a mixture state. For the first two cases, the temperature can be computed with the Newton`s method based on the enthalpy [21]. The exemplary equations for the first case are shown in the following. The second case use the same equations with another boundary conditions for the integration. The Newton`s method is a calculation algorithm for computing the solution of the function [21]. Therefore, the overall particle enthalpy is subtracted from the enthalpy equation (see equation 9). The new temperature for the next iteration step can be calculated with equation 11.

$$\boldsymbol{f(T) = h_0 + m_{O2}\int_{T_0}^{T} c_{p,O2}dT + m_{H2O}\int_{T_0}^{T} c_{p,H2O}dT + m_{H2O2}\int_{T_0}^{T} c_{p,H2O2}dT - h_{tot}} \quad \textbf{(9)}$$

$$\boldsymbol{f'(T) = m_{O2}c_{p,O2}(T) + m_{H2O}c_{p,H2O}(T) + m_{H2O2}c_{p,H2O2}(T)} \quad \textbf{(10)}$$

$$\boldsymbol{T_{new} = T - \frac{f(T)}{f'(T)}} \quad \textbf{(11)}$$

For the third case, the phase diagram has to be used to calculate the concentrations of the gaseous and the liquid part of the particle. First, a second order polynomial equation for the boiling temperature and a third order polynomial for the condensation equation is set. With the temperature of the first iteration step, the concentration can be calculated over a zero-point finding method. For the second order polynomial equation, the pq-formula can be used. For the third order polynomial equation the formula of Cardano [22] is applied. Thereby, the enthalpy can analogically to equation 9 be calculate by the bisection method [21], which leads iterative to the temperature.

2.2.3 Pressure drop

The pressure drop is usually calculated with the momentum conservation equation. Due to the complexity, that the interfacial friction depends on the interfacial area and relative velocity of the different phases [10], the momentum equation is replaced with an empirical equation for the pressure drop: the Ergun equation [23]. By reason of high Reynolds numbers, the extension of the Ergun equation from Tallmadge can be used. The formulation is shown in equation 12 [24].

$$\boldsymbol{\frac{\Delta p}{L} = \left(\frac{150}{Re} + \frac{4.2}{Re^{1/6}}\right)\frac{(1-\varepsilon)}{\varepsilon^3}\frac{\rho v^2}{d}} \quad \textbf{(12)}$$

$$\boldsymbol{Re = \frac{d\rho v}{(1-\varepsilon)\mu}} \quad \textbf{(13)}$$

Here, Δp is the pressure drop, L the catalytic bed length, Re the Reynolds number, calculated with equation 13, ε the void fraction volume, d the particle diameter and μ the dynamic viscosity. The pressure drop is the sum of the viscous and the kinetic energy losses [23].

2.2.4 Flow parameter

The mixture flow properties Φ_m are calculated with a weighted average of the liquid Φ_l and the gaseous Φ_g properties.

$$\boldsymbol{\Phi_m = (1-\chi)\Phi_l + x\Phi_g} \quad \textbf{(14)}$$

$$\boldsymbol{\Phi_l = m_{H2O2}\Phi_{H2O2} + m_{H2O}\Phi_{H2O}} \quad \textbf{(15)}$$

$$\boldsymbol{\Phi_g = m_{H2O}\Phi_{H2O} + m_{O2}\Phi_{O2}} \quad \textbf{(16)}$$

DOI: 10.13009/EUCASS2023-861

The symbol Φ is an arbitrary flow parameter and χ is the steam content. First, the averaged properties of each phase have to be computed. These average calculations are made with the mass fraction *m* of the different chemical components.
The density of the chemical components is calculated with the ideal gas equation (equation 17). For the calculation of the thermal conductivity λ, the dynamic viscosity and the heat capacity the equations used in the CEA Source Code are applied [25]:

$$\boldsymbol{\rho = \frac{p}{R_{spec}T}} \tag{17}$$

$$\boldsymbol{\ln(\lambda) = l_1 \ln(T) + l_2 T^{-1} + l_3 T^{-2} + l_4} \tag{18}$$

$$\boldsymbol{\ln(\mu) = e_1 \ln(T) + e_2 T^{-1} + e_3 T^{-2} + e_4} \tag{19}$$

$$\boldsymbol{c_p = c_1 T^{-2} + c_2 T^{-1} + c_3 T^{0} + c_4 T^{1} + c_5 T^{2} + c_6 T^{3} + c_7 T^{4}} \tag{20}$$

The coefficients l_1 to l_4, $e_1$to e_4 and $c_1$to c_7 are constants, which can be determined from data of the NIST chemistry WebBook [26]. For hydrogen peroxide only data from Coker [20] are available at higher pressures. These data have partially a different polynomial approach. Details can be seen here [20].

2.2.5 Heat transfer

For the calculation of the heat flows, the temperature of the catalytic chamber wall has to be computed first. Therefore, a two-dimensional heat equation inside of the wall is used. The wall has a spatial discretisation in the flow direction (*x*-coordinate) and a spatial discretisation normal to the flow direction (*y*-coordinate) (see figure 4). To reduce the problem, the circumferential direction is neglected. In equation 21 the heat conduction equation in two-dimensional form is shown [27]. Dirichlet boundary conditions are applied. The environmental temperature and the temperature of the fluid within the catalytic chamber are used.

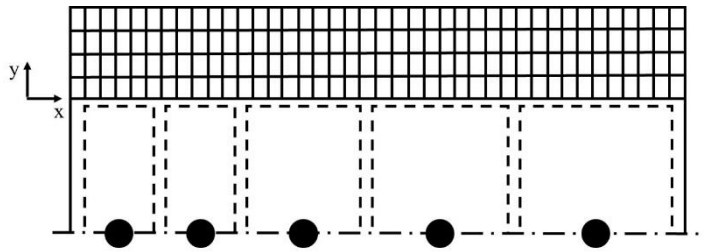

Figure 4: Wall grid

$$\boldsymbol{\frac{\partial T}{\partial t} = \frac{\lambda}{\rho c_p}\left(\frac{\partial^2 T}{\partial x^2} + \frac{\partial^2 T}{\partial y^2}\right)} \tag{21}$$

First, the temperature of the flow has to be transformed from the particle-based system to the wall grid. Then the heat conduction in the wall can be computed with the heat equation. Finally, the temperature from the wall grid has to be retransformed to the particle-based system.
The heat flow from the wall to the fluid and the heat flow from the catalytic particle to the fluid can now be calculated. With the Fourier`s law the heat flow equation is the following [27]:

$$\boldsymbol{\frac{\partial Q}{\partial t} = \alpha\,(T_2 - T_1)\,S} \tag{22}$$

Hereby, *Q* is the net heat energy transfer, α is the heat transfer coefficient, which can be calculated for the flow with the Nusselt number and *S* is the transfer area between the fluid and the solid. The transfer area of the wall with the fluid results from the surface area of a cylinder. The transfer area between the catalytic particle and the fluid results from the ratio particle surface to particle volume.

DOI: 10.13009/EUCASS2023-861

3. Exemplary results

To illustrate the application of the submodule SHAKIRA, some exemplary results of an assumed catalytic chamber are shown. In figure 5, the temperature of the particle over the particle position in the catalytic chamber is shown at a time of one second after calculation begin. Each point in the diagram is one particle in the chamber. It can be seen that the particles at the beginning are closer to each other in comparison to the end. This results from the different velocities in the chamber. Upstream the velocity is lower than downstream because the density of the fluid decrease. The temperature rises with the forward position in the chamber. At the inlet the temperature of the particle is the ambient temperature and the aggregate condition is full liquid. With the temperature increase the two-phase condition is achieved at the temperature plateau. Then the full gaseous state is reached and the temperature increase more to the steady state decomposition temperature which depends on the high-test peroxide concentration. If the last particle in the chamber is observed over the time, the temperature values at the beginning of the combustion chamber are known. In figure 6, the mass fractions of the species H_2O_2, H_2O and O_2 are displayed over the particle position. The particle positions of figure 5 and 6 are the same. At the inlet of the catalytic chamber the high-test peroxide in aqueous solution has the start concentration. First the decomposition of the high-test peroxide starts slowly. After some particle positions, the H_2O_2 mass fraction decreases fast and the mass fraction of H_2O and O_2 increase. At the outlet of the catalytic chamber the mass fraction of H_2O_2 is equal to zero and the high-test peroxide is fully decomposed. A mixture of gaseous H_2O and O_2 is injected in the combustion chamber.

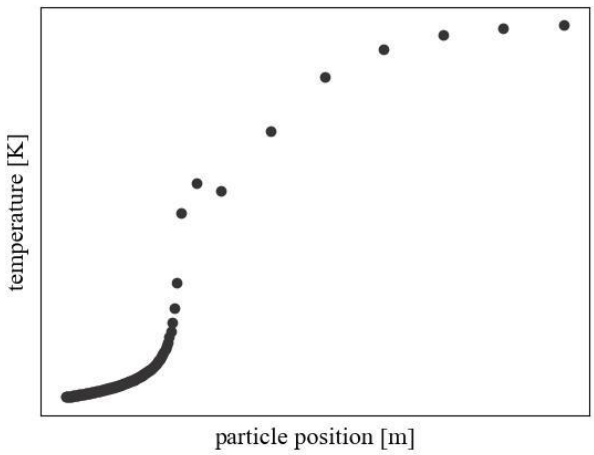

Figure 5: Temperature over particle position for a fictional catalytic chamber after one second

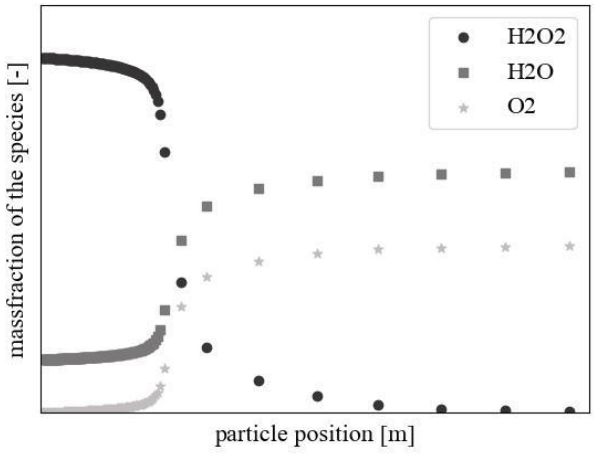

Figure 6: Mass fraction of the species over particle position for a fictional catalytic chamber after one second

Figure 7 shows the increasing wall temperature over time at the inner surface. The points in the diagram are not equivalent to the particles: they represent nodes in the wall grid. Therefore, every point has the same distance to each

DOI: 10.13009/EUCASS2023-861

other. At the time of zero seconds the wall has the ambient temperature. With increase in time, the temperature at the boundary wall increases too.

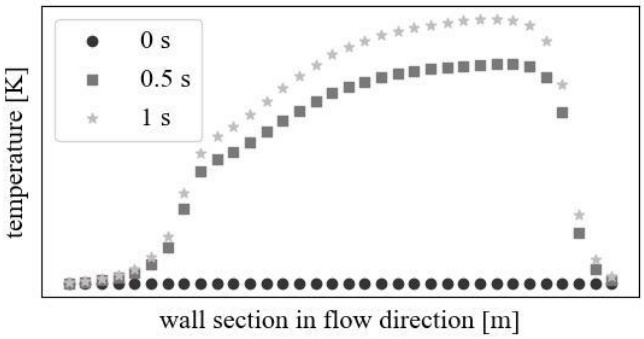

Figure 7: Temperature profile at the wall boundary for different times

4. Conclusion

To sum up this paper, a particle-based mathematical model of the flow in a catalytic chamber is presented. The model uses a simple decomposition design and an enthalpy approach for the temperature calculation. Further, a heat conduction in the wall is implemented. Exemplary results from a fictional catalytic chamber are shown.
With the presented model the decomposition of high-test peroxide in a catalytic packed bed can be simulated. The particle-based formulation opens the opportunity to study the unsteady temperature rise in the chamber before experimental tests. This is very important because it is a relevant value for the ignition delay in the engine. The temperature development for example can be applied as input value for a program to calculate the ignition delay time of a hybrid rocket engine. With the mass fraction of the components known to every time the catalytic bed length can be designed in optimal matter for best performance of the catalytic chamber. Consequently, the particle-based approach offers new opportunities in contrast to the steady-state description.
For a more detailed description of the chemical kinetics, the micro kinetics mechanism has to be taken into account. Therefore, the adsorption and desorption as well as the diffusion limitations have to be considered. Also, the homogenous description is an issue for the pressure drop calculations. As next step, it will be studied, if a heterogenous particle-based approach is possible.

Nomenclature

Latin Symbols

A	preexponential factor	$m^3/(kg\ s)$
a, b, c	constants	-
c_p	heat capacity	$J/(K\ kg)$
c_1	constant	$J\ K/kg$
c_2	constant	J/kg
c_3	constant	$J/(K\ kg)$
c_4	constant	$J/(K^2\ kg)$
c_5	constant	$J/(K^3\ kg)$
c_6	constant	$J/(K^4\ kg)$
c_7	constant	$J/(K^5\ kg)$
d	particle diameter	m
E_a	activation energy	J/mol
$e_1 – e_4$	constants	diverse
h	specific enthalpy	m^2/s^2
i	reaction order	-
k	reaction velocity	$m^3/(kg\ s)$
L	length	m
l_1 - l_4	constants	diverse
m	mass fraction	-
p	pressure	$kg/(m\ s^2)$

DOI: 10.13009/EUCASS2023-861

Q	net heat flux	W
q	heat flux	W/m^2
R	universal gas constant	$kg\ m^2/(s^2\ K^1\ mol^1)$
R_{spec}	specific gas constant	J/(kg K)
Re	Reynolds number	-
S	transfer area	m^2
s	scaling factor	-
T	temperature	K
t	time	s
v	velocity	m/s
x	axial direction	m
y	vertical to the axial direction	m

Greek Symbols

α	heat transfer coefficient	$W/(m^2\ K)$
Δ	difference	-
ε	void fraction volume	-
λ	thermal conductivity	W/(m K)
μ	dynamic viscosity	kg/(m s)
ρ	density	kg/m^3
τ	shear stress	N/m^2
Φ	arbitrary variable	-
χ	steam content	-

Subscripts

g	gaseous
H_2O	water
H_2O_2	hydrogen peroxide
l	liquid
m	mixture
new	start for the next iteration
O_2	oxygen
tot	total
0	initial

References

[1] Dadieu, A., R. Damm, E. W. Schmidt. 1968. Raketentreibstoffe. Springer-Verlag/Wien.

[2] Rocketdyne. 1967. Hydrogen Peroxide Handbook. Technical Report AFRPL-TR-67-144. United States Air Force.

[3] Bozic, O., D. Pormann, D. Lancelle and A. Hartwig. 2012. Program AHRES and its contribution to assess features and current limits of Hybrid Rocket Propulsion. International Astronautical Congress.

[4] May, S. and O. Bozic. 2015. CFD Simulation of Chemical Non-Equilibrium Reacting Flow within the AHRES Hybrid Rocket Engine. 6th European Conference for Aeronautics and Space Science (EUCASS).

[5] May, S. 2013. Mathematical Modeling of a High Test Peroxide Catalyst Chamber for Hybrid Rocket Engines. 13th ONERA-SLR Aerospace Symposium.

[6] Bozic, O., D. Pormann, D. Lancelle and S. May. 2014. The last achievements in the development of a rocket grade hydrogen peroxide catalyst chamber with flow capacity of 1kg/s. Space Propulsion.

[7] Pasini, A., L. Torre, L. Romero, A. Cervone and L. d´Agostino. 2010. Reduced-Order Model for H2O2 Catalytic reactor Performance Analysis. *Journal of Propulsion and Power*. 26:446-453.

[8] Jung, S., S. Choi, S. Heo and S. Kwon. 2021. Scaling of catalyst bed for hydrogen peroxide monopropellant thrusters using catalytic decomposition modeling. *Acta Astronautica* 187:167-180.

[9] Kerr, D.H., A.R. Karagozian, D. Bilyeu and D. Eckhardt. 2021. Nondeterministic Analysis of Monopropellant Catalyst Bed Model. *Journal of Propulsion and Power*. 37:126-138.

DOI: 10.13009/EUCASS2023-861

[10] Koopmans, R.-J., J.S. Shrimpton, G.T. Roberts and A.J. Musker. 2013. A one-dimensional multicomponent two-fluid model for reacting packed bed including mass, momentum and energy interphase transfer. *International Journal of Multiphase Flow*. 57:10-28.
[11] Reid, S., D. Symons and M. Watson. 2022. Transient, Multiscale, Heterogenous Model of Hydrogen Peroxide Decomposition for 3D-Printed Catalysts. *Journal of Propulsion and Power*.
[12] Wallis, G. B.1969. One-dimensional Two-phase Flow. McGraw-Hill Book Company.
[13] Ishii, M, T. Hibiki. 2006. Thermo-fluid dynamics of two-phase flow. Springer Science and Business Media.
[14] Walter, H. 1964. Studie über die Anwendung von hochkonzentriertem Wasserstoffperoxid als Oxidator in Drittstufen des ELDO-Trägersystems und auf weiteren Gebieten der Raumfahrt.
[15] Reschetilowski, W. 2021. Handbuch Chemischer Reaktoren. Springer Spectrum.
[16] Kieke, M. 2017. Implementation of extended chemical and geometrical calculation models in the DLR-code AHRES-SHAKIRA. Student Thesis. Technische Universität Braunschweig, Fakultät für Maschinenbau.
[17] Pirault-Roy, L., C. Kappenstein, M. Guérin and R. Eloirdi. 2002. Hydrogen Peroxide Decomposition on Various Supported Catalyst Effect of Stabilizers. *Journal of Propulsion and Power*. 18:1235-1241
[18] DIN ISO 9277. 2014. Determination of specific surface area of solids by gas adsorption – BET method.
[19] Hatanaka, K. and Y. Shibauchi. 1989. Sterilization method and apparatus therefor. United States Patent 4.797.255.
[20] Coker, A.K. 2010. Ludwig`s Applied Process Design for Chemical and Petrochenical Plants Vol. 2. Elsevier.
[21] Arens, T., F. Hettlich, C. Karpfinger, U. Kockelkorn, K. Lichtenegger, H. Stachel. 2015. Mathematik. Springer Spectrum.
[22] Irving, R. 2013. Beyond the Quadratic Formula. American Mathematical Society.
[23] Ergun, S. 1952. Fluid flow through packed columns. *Chemical Engineering Progress*. 48:89-94.
[24] Tallmadge, J.A. 1970. Packed-Bed Pressure Drop – An Extension to Higher Reynolds Numbers. *AlChE*:1092-1093
[25] Gordon, A., B.J. McBride. 1994. Computer Program for Calculation of Complex Chemical Equilibrium Compositions and Applications. I. Analysis. NASA Reference Publication 1311.
[26] Eds. Linstrom, P.J. and W.G. Mallard. NIST Chemistry WebBook. NIST Standard Reference Database Number 69. https://doi.org/10.18434/T4D303 (retrieved 11.06.2023)
[27] VDI e.V. 2013. VDI-Wärmeatlas. Springer Vieweg.